Polymerization-Filled Composites Prepared with Highly Active Filler-Supported Al/Ti/Mg Catalysts. II. Properties of Homogeneous Polyethylene-Based Composites

FRANÇOIS HINDRYCKX,[1] PHILIPPE DUBOIS,[1] ROBERT JEROME,[1] PHILIPPE TEYSSIE,[1] MIGUEL GARCIA MARTI[2]

[1] University of Liège, Center for Education and Research on Macromolecules (CERM), Sart-Tilman, B6, 4000 Liège, Belgium

[2] DOW Benelux N.V., Terneuzen, The Netherlands

Received 19 June 1996; accepted 24 September 1996

ABSTRACT: Polyethylene-based composites have been prepared by ethylene polymerization with a Al/Ti/Mg catalyst previously deposited on the surface of kaolin (Satintone W/W and Satintone 5) or barite.[1] Molecular weight (M_w) of the polyethylene matrix has been estimated from melt viscosity under steady shear flow and compared to the value measured by size exclusion chromatography. Tensile stress and strain, Young modulus, and impact energy have been measured in relation to the matrix molecular weight and the filler content. The effect of the main polymerization parameters, such as the Al/Ti/Mg composition, the addition of a transfer agent, e.g., an α-olefin or hydrogen, have also been investigated. These tensile and impact properties have been compared to composites of the same composition but prepared by melt blending of the filler and the preformed polyolefin. As a rule, the polymerization-filled composites have an improved mechanical strength compared to the analogues prepared by melt blending.
 J Appl Polym Sci **64:** 439–454, 1997

Key words: polymerization-filling technique; supported catalysts; polyethylene; homogeneous composites; mechanical properties

INTRODUCTION

Synthesis of homogeneous polyethylene-based composites by a highly active Al/Ti/Mg catalyst anchored on the surface of a mineral filler has been previously reported.[1] A catalyst efficiency as high as 300 kgPE/(gTi × h) has been observed for a Al/Ti/Mg catalyst of a 120/0.75/10 molar composition and deposited onto kaolin particles (Satintone W/W). The addition of transfer agent such as hydrogen or 1-octene has proved to efficiently control the matrix molecular weight. For instance, melt indices of 32 wt % (15 vol %) kaolin containing composites have been varied in the range from 0.01 g/10min up to 2.1 g/10 min when measured with a 2.16 kg load (MI_2).

Although the MI_2 values remain low, these polymerization-filled composites (PFCs) can be processed and shaped into articles by standard processing techniques. The polymerization-filling process is an alternative one-step route to composites containing uniformly dispersed fillers in a wide composition range from 5 wt % to 95 wt %. It is noteworthy that the highly filled composites prepared by this technique cannot be produced by melt blending the preformed polyethylene and the filler. In the early 1980s, ultrahigh molecular weight polyethylene (UHMWPE) was synthesized from a filler-supported catalyst and showed an unusual combination of high stiffness and high impact resistance even for a filler content as high

Correspondence to: Philippe Dubois.
 CCC 0021-8995/97/030439-16

as 60–70 wt %.[2–4] In spite of these valuable mechanical performances, the interest in these UHMWPE composites was limited by a very poor processability, either by compression moulding at high temperature or by blending with low molecular weight polyethylene so as to reach an acceptable melt viscosity. The latter strategy was used in Russia for producing the "Norplastic" composites.[4,5]

The mechanical properties of polymerization-filled UHMWPE composites have been reported for different types of mineral fillers such as chalk,[6,7] kaolin,[8–10] talc,[11] calcium carbonate,[12] calcium sulfate,[13] and perlite.[9] As a rule, the elongation at break decreases when the filler content is increased. No information has, however, been made available on the possible dependence of the mechanical performances on size, shape, and dispersion degree of the filler, the filler–matrix interfacial adhesion, and the matrix molecular weight.

This article aims at at least partly filling this gap. Special attention will be paid to the impact and tensile properties of polymerization-filled composites in relation to the polyethylene molecular weight, the catalyst composition, the filler content, and the main characteristics of the filler (chemical composition, shape, and size). The tensile and impact properties will be related as closely as possible to the known models for composites.[15–22] They will be compared to the composite analogues prepared by melt blending.

EXPERIMENTAL

Polymerization-filled composites were prepared in a batch reactor at 60°C, as reported elsewhere.[1] A $(BuO)_4Ti/BuMgOct/EtAlCl_2/Et_3Al$ system was anchored onto the surface of a deaggregated inorganic filler. Hydrogen (99.999%, 0–6 bar) was used as received, and ethylene (99.5%, 4 bar) was previously dried on 4 Å molecular sieves. 1-Octene (99%, Aldrich) was dried overnight over alumina previously activated by heating at 240°C for 24 h, further treated overnight with powdery CaH_2 and freshly distilled under vacuum just prior to use.

The main characteristics of kaolin (Satintone W/W and Satintone 5; Engelhard Co.) and barite (Blanc fixe N; Sachtleben) were reported in the first article in this series.[1]

For the sake of comparison, the commercially available Translink 445 (Engelhard Co.) was melt blended with neat polyethylene (Table I). Translink 445 is an aminosilane treated kaolin of the same average particle size (1.4 μm) as Satintone W/W.

Polyethylene (HDPE) of various molecular weights were used in a combination or not with 10 wt % of maleic anhydride grafted PE (MAGPE) as detailed elsewhere.[23] Melt blending was carried out with a two-roll mill in the presence of Irganox 1010 (Ciba-Geigy) at 190°C for 5 min. Samples for tensile and impact testing were cut out of 2-mm thick plates prepared by compression molding at 200°C.

Tensile properties were measured at room temperature with an Instron universal tensile tester (model DY24) in accordance with the ASTM D638 test. The gauge length was 20 mm and the crosshead speed 20 mm/min. From the stress–strain curves, the following properties (based on the average of five samples) were calculated: Young's modulus (E, GPa), yield strength (σ_y, MPa) and yield elongation (ϵ_y, %) (at the first maximum), ultimate tensile strength (σ_r, MPa) and elongation at break (ϵ_r, %).

Charpy impact tests were carried out at room temperature with a 4J hammer in order to break U-notched samples in accordance with the ASTM D 256 B test procedure. The impact energy (I.E.) was the average of five samples of 50 mm length, 6 mm width, 2 mm thickness, and 0.35 mm notch depth. Impact energy, I.E., is given in kJ/m^2.

The melting endotherms were measured with a Dupont 2000 calorimeter. Melting temperature (T_m) and degree of crystallinity (X_c) were reported from the first heating scan (T_{m1}, X_{c1}) and from the second scan recorded after sample quenching in liquid nitrogen (T_{m2}, X_{c2}). The heating rate was 25°C/min. X_c was calculated on the basis of a melting enthalpy of 2.93 $10^5 J \cdot kg^{-1}$ for 100% crystallinity PE.[14] T_m was reported as the temperature at the maximum of the melting endotherm.

Melt flow measurements were carried out at 190°C with a CEAST 6542 apparatus, according to the ASTM D 1238 norm. Three different loads were used: 2.16, 10.00, and 21.60 kg, as referred to as MI_2, MI_{10}, and MI_{21}, respectively. The results was expressed in g/10 min. The MI_{10}/MI_2 ratio was referred to as the melt flow ratio (MFR).

The filler content was calculated from the ash weight released by a well-known amount of composite (ca. 0.5 g) upon air calcination at 500°C.[1]

Polyethylene was extracted from composite samples (1.0 g) with 1,2,4-trichlorobenzene (100 mL) at 160°C under stirring, followed by hot fil-

Table I Characteristics of HDPE Used in This Study

No.	Code	Producer	M_n[a] (10^{-3})	MWD[a]	MI_2 (g/10 min)
1	Eltex B 5924	Solvay Co.	12	14	0.1
2	HDPE 10062	The Dow Chemical Co.	20	3	9.4
3	MAGPE	The Dow Chemical Co.	21	3	0.1
4	Eltex B 3925	Solvay Co.	7	21	0.1
5	Eltex B 2015	Solvay Co.	10[b]	15[b]	1.2
6	A16	The Authors[c]	10–17	9–7	1.6
7	A21	The Authors[c]	9–22	8–6	2.1

[a] As determined by SEC (see Experimental section and ref. 1).
[b] From Solvay data sheets.
[c] HDPE synthesized with a high activity $MgCl_2$-supported Ti catalyst, as reported in ref. 14.

tration of the filler. No further extraction was reported to occur after 4 days.

Molecular weight ($\bar{M}_n$, $\bar{M}_w$, $\bar{M}_v$, and M_p) and molecular weight distribution (MWD) were measured in 1,2,4-trichlorobenzene with a SEC equipment operating at 140°C and calibrated with polystyrene standards (see ref. 1).

RESULTS AND DISCUSSION

The mechanical performances of high-density polyethylene (HDPE) containing 32 wt % kaolin depends on the filling technique. Figures 1 and 2 compare the elongation at break (ϵ_r) and the σ_r/σ_y ratio for a polymerization-filled composite (PFC) and the analogues prepared by melt blending with or without interfacial agent, and the corresponding unfilled matrices.

The elongation at break of the polyethylene matrix is reduced by the introduction of filler. However, the elongation at break of the PFC sample is by far higher than ϵ_r for all the unmodified blends by melt blending HDPE of different molecular weights (Table I) with 32 wt % Satintone W/W.

The same conclusion holds for the impact resistance, that is, for the PFC sample, even higher than the corresponding matrix (Fig. 3), and to a lesser extent for the σ_r/σ_y ratio (Fig. 2).

The poorest performances of the unmodified composites prepared by melt blending are observed when a HDPE of a narrow MWD and a very high melt index is processed. The filler is supposed to be easily dispersed in this matrix of a low melt viscosity very fluid at the processing temperature. A poor interfacial adhesion is also thought to be responsible for the poor performances of the melt-blended composites. In order to support this hypothesis, HDPE has been melt blended with either an aminosilane surface-treated kaolin (Translink 445) or in the presence of 10 wt % of maleic anhydride grafted PE (MAGPE). Reaction of the anhydride group of MAGPE with the surface silanol groups of kaolin are supposed to increase the filler–polymer interfacial adhesion.

Comparison of Figure 1 to Figure 3 shows that kaolin pretreatment with an aminosilane only slightly improve the mechanical properties of the composite. This pretreatment may favor the filler deagglomeration and give the small increase in the tensile properties.

In contrast to the aminosilane interfacial agent, MAGPE significantly improves the me-

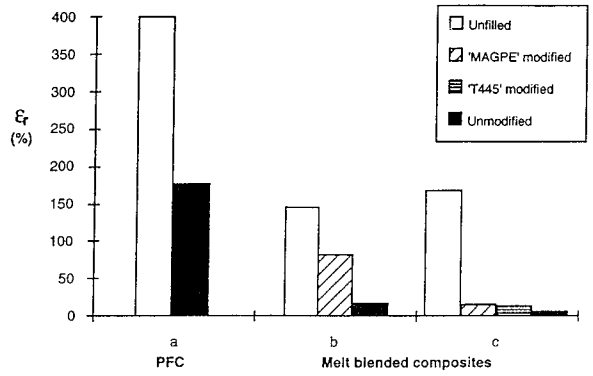

Figure 1 Elongation at break (ϵ_r) of HDPE matrices, PFC, and melt-blended composites with unmodified and modified fillers (32 wt % kaolin). Code: (a) PFC B36 unfilled (after filler removal by HF treatment) and PFC B36 (entries 1 and 2, Table IV); (b) melt-blended composites: D/0.00 matrix, D/0.15 (modified with 10 wt % of MAGPE), D/0.14 (unmodified) (entries 20, 23, and 22, Table II); (c) B/00 matrix, C/0.15 (modified with 10 wt % of MAGPE), B/0.15 (modified kaolin Translink 445), B/0.15 (unmodified) (entries 6, 17, 11, and 10 in Table II).

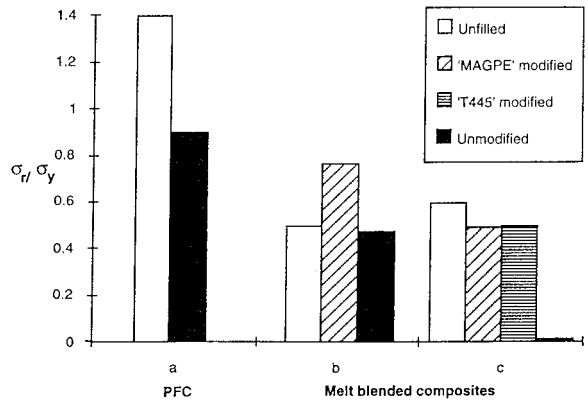

Figure 2 Tensile strength ratio (σ_r/σ_y) of HDPE matrices, PFC, and melt-blended composites with unmodified and modified fillers (32 wt % filler; code: see Fig. 1).

chanical performances, as shown in Figures 1–3. As discussed elsewhere,[23] this effect must result from the strong anchoring of the filler particles to the matrix due to the entanglements of the MAGPE chains attached to the filler within the matrix HDPE chains. Comparison of b and c indicates that this effect is more effective for a matrix of broader molecular weight distribution and, thus, of a higher weight average molecular weight (M_w is two times higher in blend b compared to blend c). From the experimental data collected in Figures 1–3, it appears that a combination of several beneficial parameters, such as filler dispersion, interfacial adhesion, and HDPE molecular weight would be at the origin of the superiority of the PFCs over the melt-blended analogues. Indeed, quite similarly to the aminosilane treatment, the catalyst preparation reacts to the surface silanol groups of the filler with an organometallic compound in such a way that the filler is deagglomerated as supported by sedimentation experiments, i.e., a sharp increase in the sedimentation time upon addition of triethylaluminum to the filler slurry in an hydrocarbon.[1]

The alkylation of the filler surface as a result of the deposition of the Al/Ti/Mg catalyst makes the filler particles less hydrophilic, and thus prone to be wetted by the HDPE chains growing from their surface. In addition to an increased filler–polymer interfacial adhesion, the coating of the filler particles by the growing polymer chains must prevent these particles from reagglomerating. Finally, the HDPE molecular weight might also influence the PFC mechanical performance.

All these results are now discussed in more detail and in relation to some predictive models.

STRESS–STRAIN PARAMETERS

Young Modulus

Inorganic fillers are currently added to polymers for manifold purposes, such as increase in stiffness (modulus), strength, impact resistance and dimensional stability, modified electrical properties, decrease in liquid and gas permeability, and cost reduction.[24]

The tensile parameters have been extracted from the stress–strain curves and listed in Tables II–IV. These data have been plotted as the ratio of the property for the composite (subscript c) to the property for the unfilled polyethylene matrix (subscript p) vs. the filler content (volume fraction, φ). The main characteristics of the HDPEs used in this study are listed in Table I. In case of PFCs, the mechanical properties of the polyethylene matrix can only be measured after the removal of the filler particles. However, because of the limited amount of PFC available, no systematical determination of the matrix molecular weight could be achieved. For this purpose, a powdery PFC sample, which is characterized by very high mechanical performances (entry 2, Table III), has been reacted with hydrofluoric acid, which leaves the HDPE matrix containing less than 2 wt % of filler (entry 1, Table III).

Modulus, which is a bulk property, mainly depends on size, shape, and concentration of the filler particles.[25] The modulus of composites is usually discussed on the basis of theories originally developed for the viscosity of suspensions,[24] because the filler particles restrict the chain and thus increase the rigidity of the matrix.

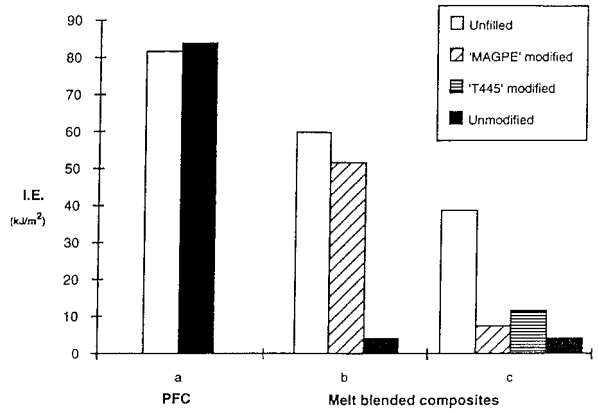

Figure 3 Impact energy of HDPE matrices, PFC, and melt-blended composites with unmodified and modified fillers (32 wt % filler; code: see Fig. 1).

Table II Filler Content, Tensile, and Impact Properties and MI of Melt Blended Composites. MW as Calculated from Melt Viscosity [eqs. (10)–(15)] and SEC

No.	Code	Filler wt %	E	σ_y	ε_y	σ_r	ε_r	I.E.	MI_2	MI_{10}	M_w ($\cdot 10^{-3}$) (MI_{10})	M_w ($\cdot 10^{-3}$) (SEC)
1	A/0.00	0	0.7	22.9	9	14.4	147	60	0.1	1.6	177	155
2	A/0.02	5	1.2	26.5	8	13.5	238	64	0.1	1.2	177	
3	A/0.05	14	1.4	25.4	7	13.7	77	32	0.1	1.2	177	
4	A/0.10	25	1.6	27.6	5	13.3	30	9	0.1	1.0	172	
5	A/0.20	40	2.2	34.9	5	18.4	25	9	0.0	2.5	172	
6	B/0.00	0	1.2	29.5	7	14.3	170	39	9.4	75.0	66	71
7	B/0.03	7	1.0	30.6	6	14.8	139	24	8.4	70.0	66	
8	B/0.10	26	1.9	31.3	5	16.0	2	10	7.9	61.6	65	
9	B/0.14	30	2.1	33.8	4	27.2	14	10	7.6	58.0	65	
10	B/0.15	32	1.7	26.2	3	26.2	5	4	6.2	57.0	65	61
11[b]	B/0.15	32	2.1	31.2	5	15.4	16	12				
12	B/0.20	41	2.3	36.0	3	33.4	7	11	4.4	40.7	69	
13	C/0.00	0							8.7		56[a]	
14	C/0.03	8	1.5	30.4	6	15.2	336	15	3.7	36.8	58	
15	C/0.06	15	1.5	30.4	7	16.3	307	14	4.7	44.1	51	
16	C/0.11	26	1.7	33.1	6	17.1	25	9	1.8	23.5	59	
17	C/0.15	32	1.8	34.5	5	16.4	18	8	2.3		54	55
18	C/0.20	40	2.5	35.7	5	28.6	11	9	0.5	9.0	76	
19	C/0.22	43	2.6	36.5	5	31.0	11	10	0.3	6.6	82	
20	D/0.00	0	1.0	27.0	8	16.3	106	60	0.1	1.2	180	150
21	D/0.06	15	1.0	21.8	6	17.4	272	12	0.1	1.5	174	
22	D/0.14	31	1.7	25.7	5	12.0	30	8	0.1	1.3	174	153
23[c]	D/0.15	32	1.8	26.6	7	21.0	84	52	0.1	1.2	180	
24	D/0.16	34	2.0	27.6	5	17.4	40	12	0.1	1.3	172	
25	E/0.00	0		28.8	8	14.0	50	61	1.2		90	
26	E/0.15	32		34.4	4	7.6	7	18	0.2	4.3	123	
27	F/0.00	0		29.2		18.3	61	61	1.6	13.9	100	120
28	F/0.26	49		38.7	3	38.7	3	10	0.1	1.0	168	
29	G/0.00	0		25.5		12.5	97	61	2.1	20.6	78	124
30	G/0.33	58		36.1	3	30.1	3	10	0.0	0.6	129	
31	G/0.43	67		39.0	3	39.0	3	11	0.0	0.2	231	

Filler is Satintone W/W: A) Eltex B5924, B) Dow 10062, C) Dow 10062 + 10 wt % MAGPE,[23] D) Eltex B3925, E) Eltex B2015, F) HDPE A2,[14] G) HDPE A16[14]. Code is: HDPE A-G/filler vol fraction.

[a] M_w value calculated from MI_2 instead of MI_{10}.

[b] Aminosilane treated kaolin (Translink 445) instead of Satintone W/W.

[c] Eltex 5924 + 10 wt % MAGPE.

The Einstein–Guth–Gold (EGG) equation,[26] also designated as the Guth–Smallwood[27] equation [eq. (1)], is an interesting relationship between the composite modulus (E_c), the polymer modulus (E_p), and the volume fraction of the filler (φ).

$$E_c = E_p(1 + 2.5\varphi + 14.1\varphi^2) \qquad (1)$$

Kerner has derived eq. (2) as an alternative for eq. (1)[28]:

$$E_c = E_p\left(1 + \frac{15(1 - \nu_p)}{(8 - 10\nu_p)}\frac{\varphi}{(1 - \varphi)}\right) \qquad (2)$$

where $\nu_p = 0.35$ is the Poisson ratio for PE. In case of rigid and spherical filler particles, Cohen–Ishai[29] have proposed eq. (3).

$$E_c = E_p\left(1 + \frac{\varphi}{1 - \varphi^{1/3}}\right) \qquad (3)$$

Dependence of the Young modulus for kaolin-filled HDPE on the filler content (φ) is shown in Figure 4. At a filler volume fraction of 0.2, the composite modulus is twice the modulus of the HDPE matrix, whatever the technique used for

Table III Tensile and Impact Properties, Melt Index, and Estimated M_w for PFCs Prepared as Described in ref. 1 (see Experimental)

No.	Code	[Ti]	φ	E	σ_y	ε_y	σ_r	ε_r	I.E.	MI_{10}	MI_{21}	$\overline{M}_w$ (MI_{10})	$\overline{M}_w$ (MI_{21}) (10^{-3})	$\overline{M}_w$ (SEC)
1	B36[a]	0.75	0.01	0.9	24.8	11	35.5	402	82	0.1	0.5	395	406	217
2	B36	0.75	0.15	1.6	30.0	7	26.8	180	84	0.0_4	0.2	325	357	205
3	B51[b]	0.75	0.15	1.8	29.8	5	28.5	185	71	0.5	1.1	207	268	144
4	B116	0.75	0.34	3.1	33.5	3	33.5	3	35	—[c]	—[c]			
5	B42	1.50	0.15	1.6	27.8	4	28.1	175	77	0.0_4	0.2	384	429	300
6	B19	2.00	0.14	1.8	28.4	5	25.3	237	73	0.3	1.1	310	269	
7	A61[d]	2.00	0.26	2.2	34.5	3	31.3	9	19	—[c]	—[c]			
8	B44	3.40	0.07	1.5	26.4	7	21.9	153	65	0.2	1.7	258	252	

Catalyst composition in Al/Ti/Mg: 120/[Ti]/10, Pethylene: 4 bar, PH_2: 1.5 bar.
[a] Filler was removed by HF treatment.
[b] PH_2 = 2 bar.
[c] No melt flow.
[d] C_2H_4 used as received (without treatment over molecular sieves).

the composite production. As a rule, the experimental data fit eq. (1), which predicts higher values than the Kerner equation. Previously, some authors have proposed a linear relationship for E_c/E_p vs. φ in case of kaolin[30] and talc[31] at low filler contents ($\varphi < 0.2$). The scattering of data in Figure 4 does not allow this proposal to be rejected. That the modulus is essentially independent of the preparation method confirms that this property is not very sensitive to how far the filler is dispersed and how strong the filler–polymer adhesion is. This is clearly confirmed by Figure 5, which shows that the relative modulus of melt-blended composites is independent of the addition of MAGPE as an interfacial agent (series C compared to series B in Table II). Once again, the experimental data agree with the Guth–Smallwood equation [eq. (1)], in contrast to eqs. (2) and (3), which predict quite comparable but smaller values.

Tensile Strength at the Yield Point

The yield stress (σ_{yc}) is an important mechanical characteristic, because it indicates the maximum load that the composite can sustain without expe-

Table IV Tensile and Impact Properties, Melt Index, and Estimated M_w for PFCs Prepared as Described in ref. 1 (see Experimental)

No.	Code	$^{P}H_2$ (bar)	E	σ_y	ε_y	σ_r	ε_r	I.E.	MI_{10}	MI_{21}	$\overline{M}_w$ (MI_{10}) (10^{-3})	$\overline{M}_w$ (MI_{21})
1	B5	2.0[a]	1.5	29.7	5	32.9	164	85[b]		0.1		568
2	B7	3.0[a]	1.8	31.4	5	19.5	36	58[b]	0.0	0.2	481	417
3	B57	0.0	1.8	29.4	5	35.1	236	56				
4	B15	1.5	1.8	31.4	5	15.9	36	58	0.3	1.5	234	248
5	B51	2.0	1.8	29.8	5	28.5	185	71	0.5	1.1	207	268
6	B60	3.0	1.8	28.2	5	13.6	69	44	0.6	2.1	203	228
7	B29	4.0	1.7	29.4	5	26.7	275	102	0.4	1.7	227	244
8	B61	6.0	1.8	25.9	5	14.0	63	23	1.0	4.0	177	198
9	B42	1.5[c]	1.6	27.8	4	28.1	175	[b]	0.0	0.2	384	429
10	B52	4.0[c]	1.9	30.8	6	16.0	60	13	0.9	3.5	180	202

Catalyst composition Al/Ti/Mg: 120/0.75/10, PH_2: 0–6 bar, PC_2H_4: 4 bar, φ = 0.15 except for B7 (φ = 0.22) and B61 (φ = 0.12).
[a] C_2H_4 used as received (without treatment over molecular sieves).
[b] Underestimated value, samples bent rather than broken.
[c] Catalyst composition Al/Ti/Mg: 120/1.5/10.

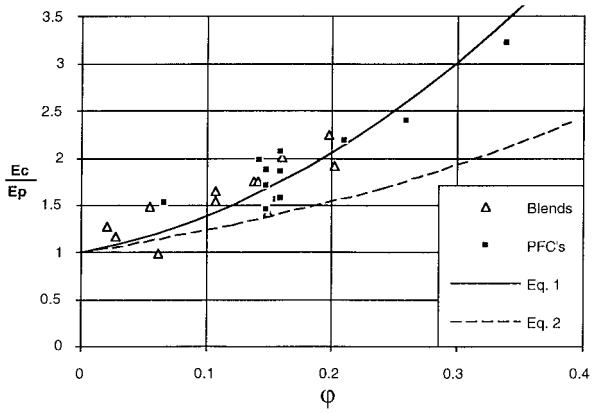

Figure 4 Dependence of the relative tensile modulus on the volume fraction of kaolin for melt-blended composites (series A, B, D–G unmodified, Table II) and PFCs, Table III). Equations (1) and (2) are also plotted for the sake of comparison.

riencing plastic deformation. The yield stress of composites depends on the complex interplay of the shape and size distribution of the filler that controls the load transfer between the filler and the matrix, the spatial distribution of the filler, and the thickness of the filler–polymer interface. Accordingly, models currently used in the composite description are not powerful enough to predict acceptable values of σ_{yc}.[32] In the extreme case of a lack of interfacial adhesion, there is no load transfer from the matrix to the particles. Then, Nicolais and Narkis[33] have derived eq. (4) for spherical particles of the same size.

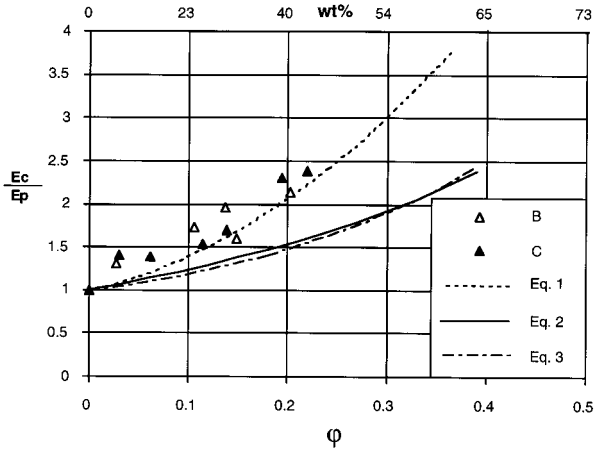

Figure 5 Effect of the interfacial adhesion on the relative tensile modulus for melt-blended composites containing MAGPE as an interfacial agent (series C, Table II) or not (series B, Table II).

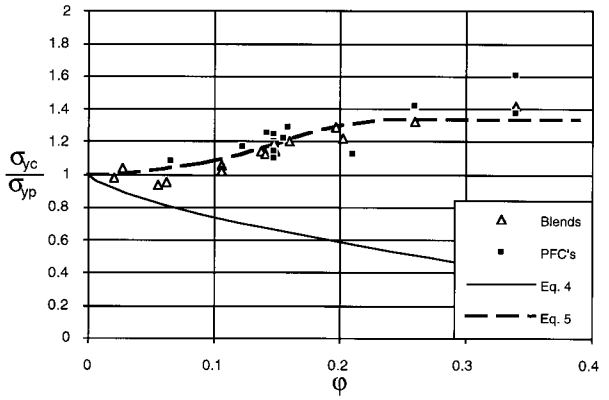

Figure 6 Dependence of the relative tensile strength at the yield point on the kaolin volume fraction (φ). Theoretical predictions by Nicolais–Narkis (eq. (4)] and Jancar [eqs. (5) and (6)] are also shown.

$$\sigma_{yc} = \sigma_{yp}(1 - (\tfrac{3}{4})^{2/3}\pi^{1/3}\varphi^{2/3}) = \sigma_{yp}(1 - 1.21\varphi^{2/3}) \quad (4)$$

In the opposite situation of an optimal adhesion, Jancar et al.[34] have proposed eq. (5) for the yield strength of filled thermoplastics.

$$\sigma_{yc} = \sigma_{yp}(1 + 0.33F\varphi^2) \quad (5)$$

where σ_{yp} is yield strength of the matrix, and F is a constant given by:

$$F = f_i; f_i = \frac{(\sigma_{yci} - \sigma^*_{yp})}{(\sigma^{\max}_{yc} - \sigma^*_{yp})\varphi_i^2} \quad (6)$$

where σ^*_{yp} is the yield strength of the matrix in the presence of a very small percentage ($\varphi < 0.03$) of filler and is the highest yield strength observed in the investigated range of φ. F is actually the average value of f_is calculated at various filler contents φ_i. For the kaolin–polyethylene system under consideration, F amounts to 25, which is comparable to the value reported for $CaCO_3$–polypropylene composites.[35]

Figure 6 shows that beyond a filler content of 0.2; thus, below a critical interparticle distance, the yield strength is maximum and levels off at a value which is 1.33 times larger than the yield strength of the HDPE matrix. The experimental data completely agree with the Jancar's model [eq. (5)]. The failure of Nicolais–Narkis model is more likely the result of the nonspherical shape and the nonidentical size of the kaolin particles.

Note that the relative tensile strength at the

yield point for melt-blended composites containing MAGPE or not is consistent with data in Figure 6 in emphasizing that the increase in the yield strength of the polymer does not significantly depend on the filler–polymer interfacial adhesion. It is then surprising that the Jancar's model accounts for the yield strength of composites melt blended in the absence of interfacial agent.

Tensile Strength at Break

The tensile strength at break largely depends on the fracture mechanism, i.e., on how far the composite sample resists the applied stress, for example, ductile or brittle fracture. This is the reason why no convenient predictive model is reported in the scientific literature.

The relative tensile strength (σ_{rc}/σ_{rp}) of PFCs and melt-blended composites characterized by a ductile fracture ($\epsilon_r > 30\%$) has been calculated. It can be noted that at a relatively high filler content (up to $\varphi = 0.25$), a ductile fracture is only observed for polymerization-filled composites. Indeed, in case of melt-blended composites, a brittle fracture mechanism occurred for filler content (φ) higher than 0.06. The strength of ductile fracture of the composites generally amounts the strength of the unfilled polyethylene ($\sigma_{rc}/\sigma_{rp} = 1$). However, the σ_{rc}/σ_{rp} data are very much scattered as various catalytic compositions have been used to prepare the PFC samples (Table III) and all were compared to the same high performance matrix, measured after filler removal (entry 1, Table III).

Yield Strain

Dependence of the yield strain (ϵ_{yc}) on the composite composition has been scarcely reported. However, this information is of interest because it deals with the transition from an elastic to a viscous behavior.

In the particular case of a good interfacial adhesion, Nielsen[36] has proposed a semiquantitative relationship between the relative elongation at break and the composite composition. Together with eq. (5), eq. (7) might be useful to predict the mechanical behavior at the yield point:

$$\epsilon_{yc} = \epsilon_{yp}(1 - \varphi^{1/3}) \qquad (7)$$

Figure 7 shows that the composites, whatever their preparation technique, qualitatively agree

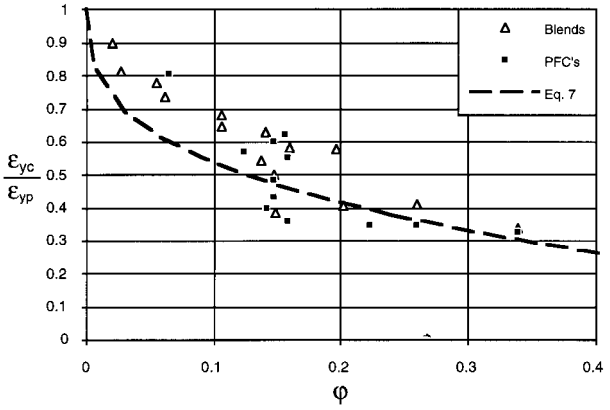

Figure 7 Relative elongation at break vs. the filler volume fraction φ. Comparison with the Nielsen's model.

with eq. (7), particularly for φ higher than 0.15. This might be explained by the relatively small strains that prevail at the yield point, keeping a good enough adhesion between the kaolin filler and the polyethylene matrix. In highly filled composites or in composites based on low molecular weight matrices, a brittle fracture mechanism is observed.

Elongation at Break

The relative elongation at break of composites compared to the unfilled matrix ($\epsilon_{rc}/\epsilon_{rp}$) significantly decreases with the increase in the filler content. The decrease is very pronounced at the low filler contents[37] (i.e., up to $\varphi = 0.15$ or 30 wt %) and then it levels off rapidly. Nielsen's model also predicts the relative elongation at break in case of ideal interfacial adhesion [eq. (8)].

$$\epsilon_{rc} = \epsilon_{rp}(1 - \varphi^{1/3}) \qquad (8)$$

The values estimated by eq. (8) are generally higher than the experimental data for the kaolin–polyethylene composites (Table III). It must, however, be noted that at very low mineral contents the elongation at break for two melt-blended composites is higher compared to the unfilled matrix. Indeed, the $\epsilon_{rc}/\epsilon_{rp}$ ratio is close to two for the A/0.02 and D/0.06 samples (entries 2 and 21 in Table II). Therefore, the few filler particles ($\varphi < 0.1$) do not initiate flaws in the ductile matrix, but rather stop the growth of flaws and cracks.

This situation is not observed for the PFC samples; the high-performance unfilled matrix used to compare all PFCs shows a very high elongation

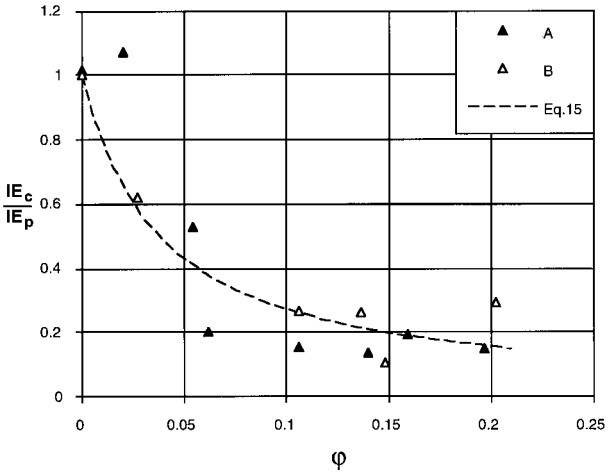

Figure 8 Dependence of the impact energy on the composition of melt-blended composites φ (series A and B in Table II).

at break (see Table III, entry 1). When the filler content is in the range of $\varphi = 0.1–0.2$, values for the relative elongation at break are widely scattered, showing the influence of the catalyst composition on the matrix molecular parameters of the PFCs. This reflects the relationship between ϵ_{rc}, the interfacial adhesion, and the molecular weight characteristics of the matrix.

The Impact Energy

The impact test is a high-speed fracture test that measures the energy to break a notched specimen. The impact energy (I.E.) is calculated from the loss of kinetic energy of a hammer-like weight pendulum according to the ASTM D256 norm (see Experimental). The Charpy impact test is performed with U-shape notched specimen, the notch of which acts as a stress concentrator so that deformation is initiated in the close vicinity of the tip of the notch.[24,38]

Figure 8 shows the dependence of the relative impact energy ($\text{I.E.}_c/\text{I.E.}_p$) on the filler volume fraction (φ) for melt-blended composites of series A (HDPE B3925) and series B (HDPE Dow 10062). I.E. rapidly decreases as the filler is added, represented by the proposed eq. (9):

$$\text{I.E.}_c = \text{I.E.}_p\left(\frac{1}{1 + a\varphi}\right) \tag{9}$$

where a is an empirical constant estimated at 27.

In case of PFCs, the relative impact strength vs. φ data leads to a complex pattern. The comparison of the I.E. of PFCs with the single unfilled matrix (entry 1, Table III) is unsuitable, and a more interesting plot should be obtained by taking into account the molecular weight parameters for each PFC sample.

Effect of the Matrix Molecular Weight on the Composites Strength

Molecular Weight Analysis

The filler usually makes the traditional analytical techniques, such as Size Exclusion Chromatography (SEC), Temperature Rising Elution Fractionation (TREF), and solution viscosity [η], unsuitable to composites. The quantitative separation of the filler from the polymer matrix is also quite a problem, which may explain why the molecular weight that is subsequently measured by SEC is smaller than expected and dependent of the sample preparation (i.e., dissolution temperature and time, filtration, . . .).[1]

A more reliable method for the molecular weight analysis is based on the steady shear flow data, i.e., the melt indices.[39,40]

The polymer molecular weight is known to depend on the melt viscosity (η_p) as follows[41]:

$$\bar{M}_w = K\eta_p^n \tag{10}$$

where K is an empirical constant that depends on the load used for the melt index measurement. K has been estimated from the comparison of molecular weight $\bar{M}_w$ as measured by SEC for the HDPE matrix of melt-blended composites (Table V) and molecular weight calculated from melt viscosity and eq. (10). Values for K and n in eq. (10) have been optimized for the calculated values to fit SEC data as closely as possible (see Table V, entries 1 and 2). There is an acceptable agreement between the molecular weight calculated from the melt indices and values collected for the polyethylene matrix, when the uncertainties on SEC data are taken into account.[1]

η_p used in eq. (10) can be calculated from the composite melt viscosity and the Einstein equation[42]:

$$\eta_c = \eta_p(1 + 2.5f\varphi) \tag{11}$$

where f is the shape factor.

The melt viscosity of a Newtonian fluid that flows through a capillary is defined as the ratio

Table V Comparison of Molecular Weight Values as Determined by SEC and from Melt Viscosity

		Size Exclusion Chromatography			Melt Viscosity		
No.	Sample	$\overline{M}_n$ (10_{-3})	$\overline{M}_w$ (10_{-3})	$\frac{\overline{M}_w}{\overline{M}_n}$	$\overline{M}_w$ (MI_2)	$\overline{M}_w$ (MI_{10})	$\overline{M}_w$ (MI_{21})
1	HDPE 10062	20	71	3.2	55	66	
2	HDPE B3925	12	155	13.7	166	171	213
3	PFC A39[a]	20	127	6.0	150	136	190
4	PFC B15	37	175	7.1		235	240
5	PFC B29	28	155	5.4		227	244
6	PFC B51	40	213	5.3	153	207	268
7	PFC B61	20	149	7.5	155	177	198

[eq. (10), $n = 0.244$ and K = 11,000, 14,000, and 18,000 for MI_2, MI_{10}, and MI_{21}, respectively]. Experimental error on SEC for unfilled (and filled) PE: $\overline{M}_n$ = 14%, (18%); $\overline{M}_w$ = 12%, (22%); $\overline{M}_w/\overline{M}_n$ = 24%, (17%).[1]

[a] Prepared from Al/Ti/Mg: 120/2.0/10 with P ethylene: 4 bar, PH_2: 1.5 bar.

of the shear stress (τ_w) and the shear rate ($\dot{\gamma}_w$ at the wall.

$$\eta_c = \frac{\tau_w}{\dot{\gamma}_w} \tag{12}$$

These data are given by eqs. (13) and (14). The shear stress at the wall of fluids that flow through a capillary is given by:

$$\tau_w = \frac{r\Delta P}{2L} \tag{13}$$

where r is the radius of capillary (1.05 mm), ΔP is the pressure difference over the capillary according to the ASTM D 1238, L is the length of the capillary (8 mm);

$$\dot{\gamma}_w = \frac{4Q}{\pi r^3} \tag{14}$$

with Q = output flow rate (m^3/s) calculated from:

$$Q = \frac{MI}{(\rho_f \phi + (1 - \phi)\rho_p)600{,}000} \tag{15}$$

where MI is the melt index (g/10 min), ρ_f and ρ_p are the filler and polymer density: 2630 kg/m^3 and 962 kg/m^3, respectively. ϕ is the filler weight fraction.

(f) has been estimated from melt-blended composites of various filler contents (Table II). Two HDPEs of a different molecular weight have been used (HDPE B5924: series A and HDPE Dow 10062: series B) and a shape factor of 3.2 ± 0.5 has been calculated. The $\overline{M}_w$ calculated from the melt indices measured for increasingly high loads are plotted as a function of the volume fraction (φ) in Figure 9. $\overline{M}_w$ is relatively constant in each series and $\overline{M}_w$ of the original HDPE reasonably fits.

$\overline{M}_w$ values have been estimated for melt-blended composites (Table II) and polymerization-filled composites and compared with SEC data in Table III and Table V. The agreement is reasonably good except for composites having a very high filler content (series F and G in Table II), and PFCs having relatively high MW, i.e., PFC B15 and B29 (Table V), for which $\overline{M}_w$ calculated from MI_{10} and MI_{21} is much overestimated, compared to SEC values. This discrepancy might confirm the inadequacy of the SEC technique for high MW determination, especially for filled com-

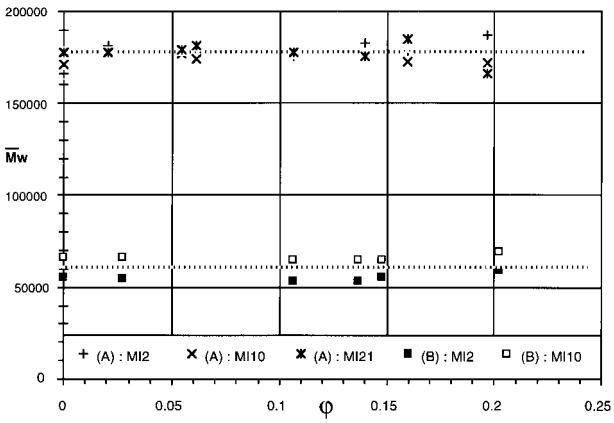

Figure 9 MW calculated from eqs. (10)–(15) and melt indices (MI_2; MI_{10} and MI_{21} for two series of melt-blended composites (series A and B in Table II).

posites. Nevertheless, the filler–polymer interfacial adhesion was not taken into account in eqs. (10)–(15). Indeed, an improved interfacial adhesion may increase the melt viscosity and, in parallel, impact energy and ϵ_r,[43] which is actually the case for PFC B15 and PFC B29 (entries 4 and 7, Table IV).

The knowledge of $\bar{M}_w$ (estimated from MI_{10}) allows now a more reliable comparison of PFCs and melt-blended composites for similar filler content.

Effect of *MW* on the (σ_{yc}/σ_{rc}) Ratio and the Elongation at Break (ϵ_{rc})

Dependence of the σ_{rc}/σ_{yc} ratio on $\bar{M}_w$ of the HDPE matrix has been plotted for both the melt-blended composites and PFCs containing ca. 30 wt % filler. When the HDPE molecular weight does not exceed ca. 350 k, an average value of 0.5 is observed for the σ_{yc}/σ_{rc} ratio. Beyond this $\bar{M}_w$, the σ_{rc}/σ_{yc} ratio sharply increases by a factor of two. This behavior has only been reported for PFCs that can accommodate much higher molecular weight HDPE compared to the analogues prepared in the melt. In this case, an exceedingly high melt viscosity prevents the filler from being properly dispersed within HDPE and forms brittle composites.

The elongation at break (ϵ_{rc}) increases with $\bar{M}_w$ for composites containing ca. 30 wt % filler ($\varphi = 0.15$) (Tables III and IV).

However, when $\bar{M}_w$ enters the range of 300 k and more, then there may be a great scattering in the data, indicating that PFCs of a high ductility can be prepared and that the catalytic compositions used to prepare the PFC samples again play an important role.[1]

Effect of MW on the Impact Energy

In good qualitative agreement with the ϵ_{rc} values, the impact energy is found to depend on the matrix molecular weight,[44] in such a way that below a $\bar{M}_w$ of 175 k the composites are very brittle, and attain a high toughness at $\bar{M}_w$ higher than 350 k (Fig. 10). The available PFCs bend rather than break, and no reliable figures can be made available.

It is clear now that the molecular weight of the HDPE matrix is one of the key parameters that control the mechanical properties of the parent composites. The remarkable superiority of the polymerization-filling technique over the conventional melt-blending procedure can be found in the production of homogeneous composites made of a high molecular weight HDPE matrix and accordingly able to attain high mechanical performances. The poor melt processability of such a high molecular weight HDPE ($\bar{M}_w \geq 300$ k) makes the preparation of toughened composites by blending difficult.

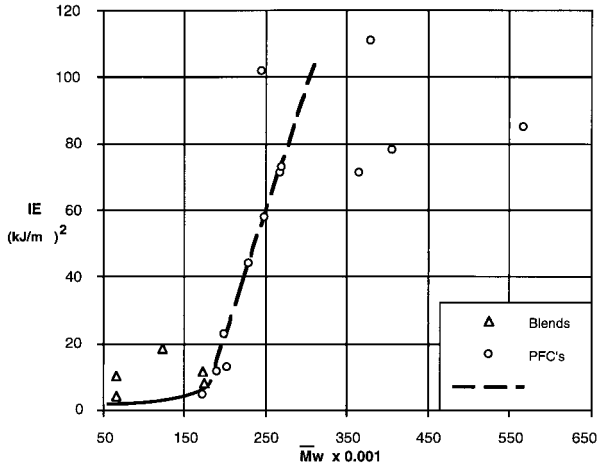

Figure 10 Dependence of the impact energy on the estimated molecular weight of the matrix for melt-blended composites and PFCs. $\varphi = 0.15$.

It is, of course, quite a problem to discriminate the beneficial effect of $\bar{M}_w$ from the effect of a possibly improved kaolin–polymer interfacial adhesion. It is worth recalling that HDPE molecular weight has been approximated from the melt viscosity on the assumption that this property is not affected by the interfacial adhesion.

The same restriction holds for the determination of the shape factor f in eq. (11). Therefore, if the interfacial adhesion is better in PFCs compared to the melt-blended analogues, it might affect the melt viscosity and value of f as well. In order to clear up this point, f has been determinated in the case of melt-blended composites modified by an interfacial agent, i.e., maleic anhydride-grafted polyethylene, MAGPE (series C in Table II). Figure 11 shows that the shape factor is increased by at least a factor of 5 when MAGPE is used, all the other conditions being the same ($f = 17.6$ instead of 3.2). A second or higher order equation will be requested for fitting the experimental data at the highest filler contents. It is thus clear that $\bar{M}_w$ as determined from the melt index of PFCs might be a crude approximation in case of a significantly improved interfacial adhesion.

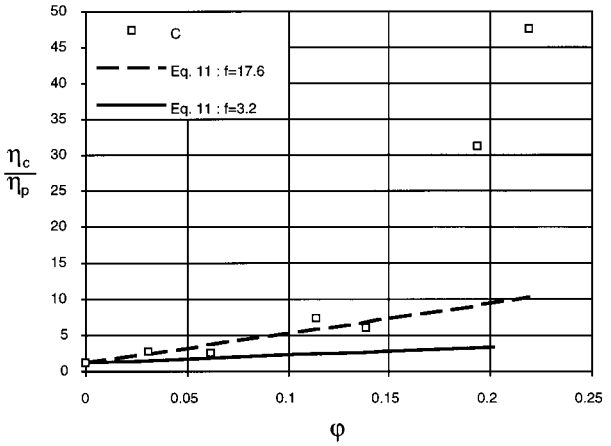

Figure 11 Determination of the shape factor in eq. (11) for melt-blended composites added with MAGPE (series C in Table II).

Effect of the Hydrogen Partial Pressure

Hydrogen has been proved to act as a chain transfer agent[1] of the ethylene polymerization. Control of $\bar{M}_w$ by H_2 is confirmed by the increase in melt indices (Fig. 12) and the parallel decrease in $\bar{M}_w$ estimated from MI (Table IV). The decrease in the HDPE chain length may be correlated with poorer mechanical properties, particularly ϵ_r and I.E. This observation is reported for two catalyst compositions (i.e., Al/Ti/Mg = 120/0.75/10, entries 1–8 and 120/1.50/10 entries 9–10 of Table IV).

Effect of 1-Octene

Composites were also synthesized in the presence of 1-octene (Table VI). At low octene–ethylene molar ratios, there is a decrease in $\bar{M}_w$ and, thus, an increase in the melt flow index, which indicates that the α-olefin mainly acts as a transfer agent rather than as a comonomer. This has been confirmed by ^{13}C-NMR analysis of the final polymer.[1] This decrease in molecular weight is unavoidably accompanied by a loss in ϵ_r combined with a σ_{yc}/σ_{rc} ratio close to 0.5. When the 1-octene–ethylene ratio is such that $\bar{M}_w$ is increased, the tendency is reversed and a ϵ_r value higher than 150% is even observed. The role played by 1-octene is rather complex and requires a more detailed study of the effect of the α-olefin on the active sites.

SEM Observations

In order to visualize the expected filler–polymer interfacial adhesion in PFCs, the fracture surfaces as produced by the tensile [Fig. 13(a)–(b)] and impact testing [Fig. 14(a)–(b)] have been observed by SEM. In case of PFC [Fig. 13(a)], small filler particles are observed that are more or less regularly distributed and interconnected through stretched polymer threads. The morphology is quite different for melt-blended composites. Much larger particles (>10 μm) are observed, which appear to be less well adhered to the matrix [Fig. 13(b)].

No filler particles can be observed on the fracture surfaces of melt-blended composites resulting from impact testing [Fig. 14(b)]. This suggests a poor adhesion between the kaolin particles and the polymer. In contrast, Figure 13(a) shows filler particles still attached to the polymeric matrix via polyethylene fibrils.

Effect of the Filler Nature

The filler nature and the particle size are also expected to be of prime importance for both the catalyst anchoring and the final mechanical properties.

Satintone 5 is also a kaolin filler but of a smaller particle size (0.8 mm) compared to Satintone W/W (1.4 mm). ϵ_{rc} and I.E. are improved as the particle size is decreased (entries 1 and 2 of Table VII at same φ). PFCs of a high Satintone 5 content (up to 50 wt %, $\varphi = 0.26$) exhibit very high ϵ_r and I.E. values and a σ_{rc}/σ_{yc} ratio higher than unity.

A still higher filler content (63 wt %, $\varphi = 0.34$) has a detrimental effect on the elongation at break and impact energy. These data demonstrate the beneficial effect of a decrease in the average

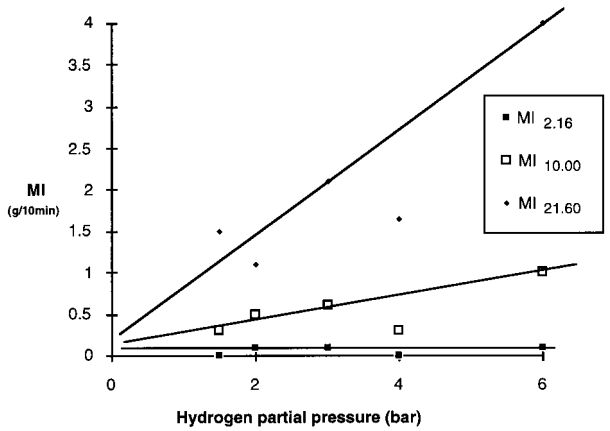

Figure 12 Dependence of the melt indices on the hydrogen partial pressure for PFCs ($\varphi = 0.15$).

Table VI Mechanical Properties, Melt Indices, and $\overline{M}_w$ for PFCs Prepared in the Presence of 1-Octene

No.	Code	Octene–ethylene ratio 10^{-3}	E	σ_y	ε_y	σ_r	ε_r	I.E.	MI_2	MI_{10}	MI_{21}	$\overline{M}_w$ (MI_2)	$\overline{M}_w$ (MI_{10}) 10^{-3}	$\overline{M}_w$ (MI_{21})
1	B64	0.0	2.1	27.1	4	27.3	271	—[a]			0.3			362
2	B55	4.0	2.3	32.0	3	16.6	36	9	0.6	3.2	13.8	102	144	147
3	B56	8.0	2.2	32.6	12	26.1	10	4	2.1	14.5	70.0	74	119	98
4	B63	12.0	1.9	30.6	6	15.0	42			0.1	0.4		551	341
5	B58	40.0	1.6	22.1	4	22.7	175	62[a]						

φ = 0.15 (32 wt %) of Satintone W/W.
[a] Could not be accurately measured.

particle size. Barite has been also tested as a filler in the PFC's production.[1] Table VII (entries 5 and 8; $\varphi \pm 0.10$) and (entries 1, 2, and 8; ±32 wt %) shows the effect of the substitution of barite for Satintone W/W in the same melt-blended composite (HDPE Dow 10062). There is a general decrease in the tensile mechanical properties of the barite-based composites.

From the comparison of entries 1 and 7 and 8 and 9 in Table VII, the superiority of the polymerization approach over the melt blending procedure is obvious. ϵ_r for PFC is as high as 430% compared to 9% of the melt-blended analogue. The more regular cubic shape of barite particles compared to anisotropic flake-shaped particles of Satintone might account for the smaller modulus observed.

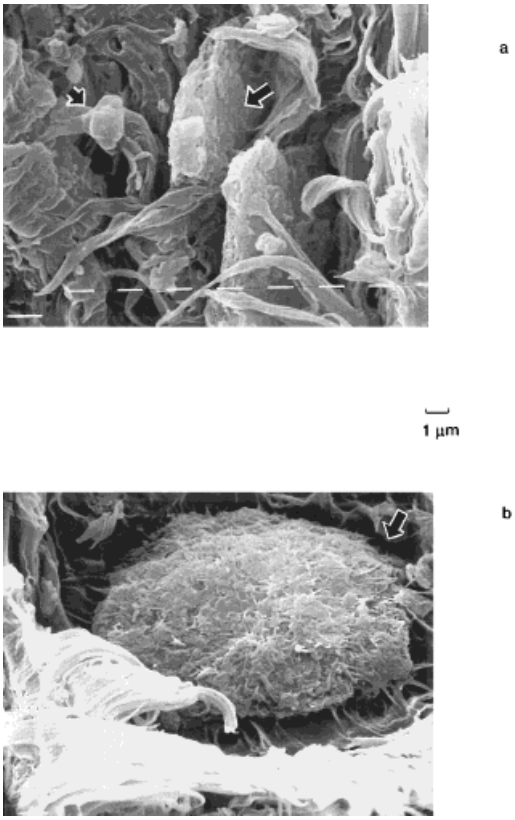

Figure 13 SEM of fracture surfaces as resulting from tensile testing: (a) PFC, (b) melt-blended composites (φ = 0.15).

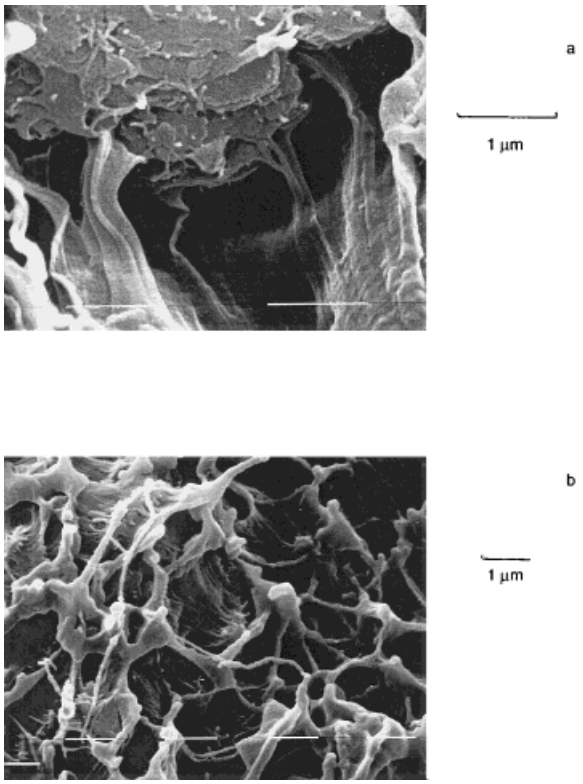

Figure 14 SEM of fracture surfaces resulting from impact testing: (a) PFC, (b) melt-blended composites (φ = 0.15).

Table VII Effect of the Filler Nature

No.	Code	Type	Sample	wt %	φ	E	σ_y	ε_y	σ_r	ε_r	I.E.
1	B/0.15	Blend	Satintone W/W	32	0.15	1.7	26	3.0	26	5	4
2	B/0.15	Blend	Satintone 5	32	0.15	2.0	32	5.3	16	34	57
3	B117	PFC	Satintone 5	52	0.26	2.7	33	3.2	39	68	145
4	B118	PFC	Satintone 5	63	0.34	3.4	22	2.4	24	3	22
5	B/0.10	Blend	Satintone W/W	25	0.10	1.9	31	5.0	16	2	10
6	B44	PFC	Satintone W/W	16	0.07	1.5	26	7.0	22	153	65
7	B36	PFC	Satintone W/W	32	0.15	1.6	30	6.8	22	180	84
8	B/0.09	Blend	Blanc fixe N	31	0.09	1.3	25	2.2	12	9	8
9	B105	PFC	Blanc fixe N	31	0.09	1.2	26	3.3	33	431	—[a]

Comparison of PFCs and melt blended composites. (HDPE 10062). PFC produced as described in ref. 1. Kaolin; density 2.63: Satintone W/W: average size 1.4 μm; Satintone 5: 0.8 μm, barite: Blanc fixe N; density 4.4: average size 3 μm.

[a] Could not be accurately measured.

CONCLUSIONS

The superiority of polymerization-filled composites (PFCs) over melt-blended composites emerges from the comparison of the impact energy (I.E.), the elongation at rupture (ϵ_r), and the σ_{rc}/σ_{yc} tensile strength ratio. This superiority is maintained even when kaolin is pretreated with an aminosilane, which is known to deagglomerate the filler particles (Translink 445: aminosilane-treated kaolin), or when the interfacial adhesion is modified by reaction of the filler with maleic anhydride grafted polyethylene. The improved mechanical performance of PFCs is thought to result from several parameters, such as fine filler dispersion, good filler–polymer interfacial adhesion, and high molecular weight of the matrix. The tensile and impact properties of PFCs have been thoroughly analyzed with reference to some predictive models and to data reported for melt-blended composites. The main conclusions can be summarized as follows. The tensile modulus (E) rapidly increases with the filler content according to the Einstein–Guth–Gold model. E is not sensitive to the technique used for the composite production, thus to the filler dispersion and the interfacial adhesion. It would, however, be dependent on the filler shape as shown by the substitution of barite for kaolin in PFCs.

At the yield point, the relative stress σ_{yc}/σ_{yp}, decreases with the filler content, in agreement with load transfer from the matrix to the filler particles, and therefore, with a good interfacial adhesion as assumed by the model of Jancar et al. Because this effect is also observed independent of the technique used for the composite production, kaolin appears to be a good reinforcing agent that imparts high stiffness to HDPE and good interfacial adhesion toward this polymer. Consistently, the elongation at the yield point is in qualitative agreement with Nielsen's model, valid in case of a high filler–polymer adhesion. The ultimate tensile strengths of PFCs match with the unfilled PFC matrix, even at relatively high filler loadings, i.e., up to 35 wt % of filler (φ = 0.16), while, in the case of melt-blended composites, a brittle behavior is observed above 15 wt % (φ = 0.06).

The elongation at break drastically decreases upon increasing filler loading, this effect being more pronounced in the case of melt-blended composites. The impact energy changes the same way at constant HDPE molecular weight. High toughness is, however, reported for PFCs when $\bar{M}_w$ is close to or higher than 300,000. In parallel, the σ_{yc}/σ_{rc} ratio sharply increases from ca. 0.5 to 1.0.

The $\bar{M}_w$ of PFC's matrix has been approximated from steady shear flow measurements, because SEC proved to be not accurate enough in case of relatively high $\bar{M}_w$s. The irregular shape of kaolin (Satintone W/W) has been taken into account [shape factor (f)] in the relationship between the melt viscosity of the composite and the parent HDPE, respectively. The shape factor has however been determined from data collected for melt-blended composites. Therefore, this value of f (3.2) might only be an approximation for PFCs because a five times higher value of f has been calculated when the melt-blended composites are modified by MAGPE.

The catalyst composition and the addition of hydrogen and 1-octene to the reaction medium can have a profound influence on the mechanical performances of PFCs, which is actually an indi-

rect confirmation of the very important role of molecular weight.

The filler nature and particle size can also contribute to the improvement of the tensile and impact property as exemplified by a decrease in the particle size of the Satintone type of filler and the use of barite instead of kaolin, i.e., a more isotropic filler.

Although direct evidence is lacking, the improved mechanical strength of the PFCs is attributed to the improved wetting of the filler by the polymer and to the filler dispersion as the result of the filler surface treatment by the catalyst components. The matrix molecular weight is clearly of a prime importance. The polymerization-filling technique has the unique capability of producing homogeneous composites of a high filler content and a high molecular weight matrix. The catalyst composition and the addition of a transfer agent allow the molecular weight of the polyethylene matrix and, thus, the mechanical performances to be controlled. High $\bar{M}_w$s are at the origin of high mechanical performances but also of high melt viscosities. Depending on the final application, the main characteristics of PFCs can be modulated by the interplay of the catalyst Al/Ti/Mg composition and the addition of hydrogen and/or 1-octene.

A straightforward comparison of PFCs with melt-blended composites is quite a problem because of the difficulty of matching the $\bar{M}_w$ and molecular weight distribution of HDPE in the two series of composites. Furthermore, PFCs have high performances in a molecular weight range where the melt processing of composites cannot be implemented anymore.

The authors are very much indebted to Dow Benelux N.V. (Terneuzen) and to the "Services Fédéraux des Affaires Scientifiques, Techniques et Culturelles" in the frame of the "Pôles d'Attraction Interuniversitaires: Polymères." Philippe Dubois is a Research Associate of the Belgian National Fund for Scientific Research (FNRS).

REFERENCES

1. F. Hindryckx, Ph. Dubois, R. Jérôme, Ph. Teyssié, and M. Garcia Marti, *J. Appl. Polym. Sci.,* to appear.
2. E. G. Howard, R. D. Lipscomb, R. N. MacDonald, B. L. Glazard, C. W. Tullock, and J. W. Collette, *Ind. Eng. Chem. Prod. Res. Dev.,* **20,** 421 (1981).
3. E. G. Howard, R. D. Lipscomb, R. N. MacDonald, B. L. Glazard, C. W. Tullock, J. W. Collette, *Ind. Eng. Chem. Prod. Res. Dev.,* **20,** 429 (1981).
4. N. S. Enikolopian, A. A. Fridman, W. L. Popov, I. O. Stalnova, A. A. Briekenstein, W. M. Rudakov, N. P. Gherasina, and A. E. Tchalykh, *J. Appl. Polym. Sci.,* **32,** 6107 (1986).
5. F. S. D'yachovskii and L. A. Novokshonova, *Russian Chem. Rev.,* **53,** 117 (1984).
6. M. Gorelik, E. A. Fushman, A. Topolkaraev, F. S. Dyachkovsky, L. A. Shestenia, L. F. Borisova, and I. Sergeev, *J. Appl. Polym. Sci.,* **40,** 1095 (1990).
7. L. Minkova and P. L. Maganini, *Polym. Degrad. Stabil.,* **42,** 107 (1993).
8. N. N. Vlasova, I. Sergeyev, P. Y. Matkovskii, N. S. Yenikolopyan, A. T. Papoyan, B. Y. Vostorgov, L. N. Grigorov, S. A. Bukanova, L. O. Bunina, N. S. Kogarko, L. A. Trachenko, and X. Smirnov, *Polym. Sci. URSS,* **27,** 2552 (1985).
9. D. Damyanov, I. Ivanov, and M. Velikova, *Eur. Polym. J.,* **24,** 657 (1987).
10. I. N. Meshkova, T. M. Ushakova, I. L. Dubnikova, Y. M. Kazakov, Y. A. Shashkova, N. M. Rudneva, N. K. Portnaya, G. N. Kornienko, A. I. Petrosyan, A. I. IMakhin'ko, and F. S. D'yachkovskii, *Polym. Sci. URSS,* **28,** 724 (1986).
11. I. L. Dubnikova, I. N. Meshkova, G. Grinev, Y. M. Tovmasyan, and F. S. D'yachkovskii, *Doklady Phys. Chem. (Engl. Transl. of Dokl. Akad. Nauk SSSR,* **281,** 629 (1985).
12. Q. Fu and G. Wang, *J. Appl. Polym. Sci.,* **49,** 1985 (1993).
13. W. Schöppel and K. H. Reichert, *Makromol. Chem., Rapid Commun.,* **3,** 483 (1982).
14. F. Hindryckx, Ph. Dubois, R. Jérôme, Ph. Teyssié, and M. Garcia Marti, *Ethylene Polymerization by a High Activity $MgCl_2$ Supported Ti Catalyst in the Presence of Hydrogen and / or 1-Octene,* , to appear.
15. L. A. Vratsanos and R. J. Farris, *Polym. Eng. Sci.,* **33,** 1458 (1993).
16. S. N. Maiti and B. H. Lopez, *J. Appl. Polym. Sci.,* **44,** 353 (1992).
17. J. Jancar and J. Kucera, *Polym. Eng. Sci.,* **30,** 714 (1990).
18. Q. Fu, G. Wang, and J. Shen, *J. Appl. Polym. Sci.,* **49,** 673 (1993).
19. P. Chacko, F. E. Karasz, and R. J. Farris, *Polym. Eng. Sci.,* **22,** 968 (1982).
20. N. Morozova and A. Topolkrayev, *Polym. Sci. URSS,* **33,** 79 (1991).
21. C. G. Ek, J. Kubât, and M. Rigdahl, *Rheol. Acta,* , **26,** 55 (1987).
22. Y. C. Gao and J. Lelievre, *Polym. Eng. Sci.,* **34,** 1369 (1994).
23. F. Hindryckx, Ph. Dubois, M. Patin, R. Jérôme, Ph. Teyssié, and M. Garcia Marti, *J. Appl. Polym. Sci.,* **56,** 1093 (1995).
24. L. E. Nielsen, *Mechanical Properties of Polymers and Composites,* Vol. 2, Dekker, New York, 1974.

25. G. Akin–Öktem and T. Tinçer, *J. Appl. Polym. Sci.,* **54,** 1103 (1994).
26. E. Guth, *J. Appl. Polym. Sci.,* **22,** 3513 (1984).
27. R. D. Deanin and N. R. Schott, *Filler and Reinforcements for Plastics,* R. F. Gould, Ed., ACS Series 134, American Chemical Society, Washington, DC, 1974.
28. E. H. Kerner, *Proc. Phys. Soc.,* **69B,** 808 (1969).
29. L. Cohen and O. Ishai, *J. Comp. Mater.,* **1,** 390 (1967).
30. V. Dolàkovà-Svehlovà, *J. Macromol. Sci. Phys.,* **B21,** 231 (1982).
31. H. Kothandaraman and M. S. Devi, *J. Polym. Sci., Part A: Polym. Chem.,* **32,** 1283 (1994).
32. B. Turcsanyi, B. Pukànszky, and F. Tüdos, *J. Mater. Sci.,* **7,** 160 (1988).
33. L. Nicolais and M. Narkis, *Polym. Eng. Sci.,* **11,** 194 (1971).
34. J. Jancar, A. Dienselmo, and A. T. Dibenedetto, *Polym. Eng. Sci.,* **32,** 1394 (1992).
35. G. J. Ray, P. E. Johnson, and J. R. Knox, *Macromolecules,* **10,** 773 (1977).
36. L. E. Nielsen, *J. Appl. Polym. Sci.,* **10,** 97 (1961).
37. V. Doláková-Svehlová, *J. Macromol. Sci.-Phys.,* **B21,** 231 (1982).
38. J. G. Williams, *Fracture Mechanics of Polymers,* Ellis Howood Limited, Wiley, New York, 1984.
39. J. F. Roos, *J. Polym. Sci., Polym. Chem. Ed.,* **22,** 2255 (1984).
40. H. Verhoogt, PhD Thesis, Technische Universiteit, Delft (1992).
41. T. G. Fox, S. Gratch, and S. Loshaek, *Viscosity Relationships for Polymers in Bulk and in Concentrated Solution,* Vol. 1, Academic Press, New York, 1978.
42. A. Einstein, *Ann. Physik,* **34,** 591 (1911).
43. T. M. Malik, *Polym. Bull.,* **26,** 709 (1991).
44. V. Svehlovà, E. Polouček, *Angew. Makromol. Chem.,* **174,** 205 (1990).